Materials Chemistry and Physics 138 (2013) 559–564

Contents lists available at SciVerse ScienceDirect

Materials Chemistry and Physics

journal homepage: www.elsevier.com/locate/matchemphys

Micellization behavior of tertiary amine-methacrylate-based block copolymers characterized by small-angle X-ray scattering and dynamic light scattering

Y. Özcan [a,c], S. İde [b,*], U. Jeng [c,d,**], V. Bütün [e], YH. Lai [f], CH. Su [c,g]

[a] Pamukkale University, Faculty of Arts and Sciences, Department of Physics, 200070 Denizli, Turkey
[b] Department of Physics Engineering, Hacettepe University, 06800 Beytepe, Ankara, Turkey
[c] National Synchrotron Radiation Research Center, Hsinchu 30076, Taiwan
[d] Department of Chemical Engineering, National Tsing Hua University, Hsinchu 300, Taiwan
[e] Faculty of Arts and Science, Department of Chemistry, Eskisehir Osmangazi University, 26480, Eskisehir, Turkey
[f] Department of Chemistry, Tunghai University, Taichung 407, Taiwan
[g] Industrial Technology Research Institute, Hsinchu 310, Taiwan

HIGHLIGHTS

- Water-soluble diblock copolymers have been synthesized via GTP.
- AB diblock copolymers form B-core micelles in aqueous media at basic pH values.
- AB diblock copolymers depend on the n/m, M_w, solution temperature and solution pHs.
- By SAXS, micellization behaviors of the AB diblock copolymers were determined.

ARTICLE INFO

Article history:
Received 26 April 2012
Received in revised form
3 December 2012
Accepted 9 December 2012

Keywords:
Polymers
Light scattering
Small-angle scattering
Chemical synthesis

ABSTRACT

We have studied the micellization behavior of tertiary amine methacrylate-based diblock copolymers, comprising the hydrophobic poly[2-(diethylamino)ethyl methacrylate] (PDEA) and hydrophilic/polyelectrolyte poly[2-(dimethylamino)ethyl methacrylate] (PDMA) blocks. Revealed by small-angle X-ray scattering (SAXS) and dynamics light scattering, micelle size of the $PDMA_m$–b–$PDEA_n$ diblock copolymer in aqueous solution depends sensitively on the comonomer ratio n/m, molecular weight M_w, solution temperature, and solution pH values. Aggregation number is found to follow an empirical relation of $N \propto (n/m)^{1.6}$, disregarding the molecular mass. With $n/m = 0.5$, $M_w \approx 12{,}000$, and pH = 7.6, the diblock copolymer forms spherical core–shell micelles at 23 °C, with a PDEA-core radius of 52 Å, a PDMA-shell thickness of 27 Å, and an aggregation number of 127.

1. Introduction

Synthesis and micellization behavior of hydrophilic copolymers and their derivatives have been widely studied since 1990, because of their environment-friendly processing without organic solvent and practical applications in pharmaceutical, agricultural and cosmetic industries via supercritical fluid technologies and nano-scale engineering [1,2]. Among the studies, water-soluble copolymers based on tertiary amine methacrylates [3–12] provide rich variations and have potential for various applications due to their stimuli responsive natures. An illustrative example is the block copolymers of 2-(dimethylamino)ethyl methacrylate and 2-(diethylamino)ethyl methacrylate monomers (PDMA–*b*–PDEA) which can selectively form micelles when the solution pH is above ~7 [3,8]. Specifically, the amine groups on the side chains of the both blocks of the PDMA–*b*–PDEA copolymer are protonated under acidic environment; thereby the copolymer can dissolve in aqueous solutions as unimers due to ion-dipole attraction and behaves as polyelectrolytes. Upon increase of the pH value above ~7, deprotonation of the side chains causes the PDEA block to be dehydrated and hydrophobic due to steric effect of the two ethyl groups. Consequently the copolymers form micelles with PDEA-

* Corresponding author. Tel.: +90 312 2977248.
** Corresponding author. National Synchrotron Radiation Research Center, Hsinchu 30076, Taiwan. Tel.: +886 3 5780281x7108.
E-mail addresses: ozcan@pau.edu.tr (Y. Özcan), side@hacettepe.edu.tr (S. İde), usjeng@nsrrc.org.tw (U. Jeng).

0254-0584/$ – see front matter © 2012 Elsevier B.V. All rights reserved.
http://dx.doi.org/10.1016/j.matchemphys.2012.12.019

cores and hydrophilic PDMA-shells. We emphasize that above pH = 7 PDEA (pK_a around 7.3) undergoes conformational transition first and forms the micelle cores; further increase of pH value higher than 8.4 would result the transition of PDMA too (pK_a around 8.4), leading to phase-separation (i.e. precipitation) of the copolymer from the solution [3–12]. Micellization of the PDMA–*b*–PDEA copolymer also has responses to both salt concentration (ionic strength) in the aqueous solution and solution temperature, as illustrated previously [13]. Furthermore, inclusion of a temperature sensitive block of poly[2-(*N*-morpholino)ethyl methacrylate], PMEMA, for a triblock copolymer of $PMEMA_l$–*b*–$PDMA_m$–*b*–$PDEA_n$, one can modulate conveniently the hydrophilicity and hydrophobicity of the tertiary amine methacrylate-based triblock copolymer by temperature, resulting in thermally reversible micellization in the vicinity of human body temperature for potential drug carriers [8,14,15].

With fluorescence spectroscopy, dynamic light scattering (DLS), and small-angle neutron scattering (SANS) [10], micellization of diblock copolymer $PDMA_m$–*b*–$PDEA_n$ has been studied in detail [7–11,13–15] for the dependences of micellization on composition, structure, molecular mass, solution ionic strength or temperature. Nevertheless, the dependences of micelle size and aggregation number of $PDMA_m$–*b*–$PDEA_n$ diblock copolymers on the comonomer ratio (n/m) have not been examined systematically. In this study, using mainly small-angle X-ray scattering (SAXS), we focus on the micellization behavior of PDMA–*b*–PDEA diblock copolymer as a function of n/m ratio of the copolymer; dependences on molecular weight, concentration, and pH value of the solution are also examined. As a result, SAXS is found to provide a better scattering contrast in resolving the core–shell micelle structure of the copolymer (formed with smaller molecular mass), not differentiated in the previous SANS study [11]. DLS is also used for consistency check on the micelle size and polydispersity revealed by SAXS. The aggregation behavior observed for the copolymer micelles is discussed in terms of effective packing parameters similar to that used for surfactant micelles.

2. SAXS model

SAXS intensity distribution for colloidal particles can be modeled with

$$I(Q) = n_p P(Q) S(Q) \tag{1}$$

with the number density n_p, form factor $P(Q)$ and structure factor $S(Q)$. The wavevector transfer $Q = 4\pi\ \lambda^{-1}\ \sin\ \theta$ is defined by the wavelength λ and scattering angle 2θ. For dilute solutions with little interparticle interactions, $S(Q)$ is close to unity and may be neglected [16]. Consequently, the zero-angle scattering intensity at $Q = 0$ can be simplified to

$$I(0) = (C - C_0) N V_{dry}^2 \left(\rho_p - \rho_o\right)^2 \tag{2}$$

with the copolymer concentration C, critical micelle concentration C_o, aggregation number N, the volume of the copolymer V_{dry}, and the scattering length densities of the copolymer and solvent ρ_p and ρ_o (for water $\rho_o = 9.43 \times 10^{-6}$ Å^{-2} or 0.337 e$^-$ Å^{-3}) [16–20]. N can be deduced with the measured $I(0)$ value. Furthermore, for monodisperse core–shell micelles, the form factor $P(Q) = |F(Q)|^2$, with

$$F(Q, R_c, R_s) = \frac{4}{3}\pi\left[R_c^3(\rho_c - \rho_s)F_0(QR_c) + R_H^3(\rho_s - \rho_o)F_0(QR_H)\right] \tag{3}$$

where $F_0(x) = 3x^{-3}(\sin x - x\cos x)$ with $x = QR_c$ or QR_H. Here, R_c is the core radius; the micellar radius $R_H = R_c + t$, with the shell thickness t. Here, the scattering length densities of the core and shell are respectively ρ_c and ρ_s. Furthermore, with the polydispersity in micellar size taken into account, SAXS intensity profile becomes $I(Q) = \langle n_p \rangle \langle P(Q) \rangle$, with the averaged form factor $\langle P(Q) \rangle = \langle P(Q, r) f(r) \rangle$. The number density of the scattering particles $n_p(r) = \langle n_p \rangle f(r)$ is defined by the mean number density $\langle n_p \rangle$ and the Schultz size-distribution function [21].

$$f(r) = \left(\frac{z+1}{r_a}\right)^{z+1} r^z \exp\left[-\left(\frac{z+1}{r_a}\right) r\right] \Big/ \Gamma(z+1) \tag{4}$$

with $z > -1$, and the mean size r_a, width parameter z, and polydispersity $p = (z + 1)^{-1/2}$. For simplicity, we use the same polydispersity for the core and micelle sizes. Fig. 1 depicts a core–shell micelle with the defined structural parameters.

Micelle size can also be estimated from the radius of gyration R_g extracted from the model-independent Guinier approximation

$$I(Q) \propto \exp\left(-R_g^2 Q^2/3\right) \tag{5}$$

in the low-q regime ($R_g Q \lesssim 1$) of an SAXS profile [16].

3. Experimental

3.1. Sample preparation

A series of $PDMA_m$–*b*–$PDEA_n$ block copolymers, with n/m values ranging from 0.25 to 0.78 and a molecular weights M_w of either ~22,000 or ~12,000 g mol^{-1}, were synthesized (summarized in Table 1) as described previously [8]. Samples were dissolved in aqueous solutions in the concentration range of 5–20 mg mL^{-1}, using the process illustrated in Fig. 2. Specifically, at 23 °C block copolymer samples of various concentrations were dissolved in aqueous solutions at a pH value ca. 2–3 by adding HCl solution, followed by addition of KOH solution for the designated solution pH values (7.5–8.0) and micellization of the block copolymer. Micellization was first indicated by the color transition of the sample solutions from transparent to tint blue before SAXS and DLS measurements.

3.2. SAXS and DLS measurements

SAXS measurements were performed at the beamline 17B3 of the National Synchrotron Radiation Research Center (NSRRC) [22].

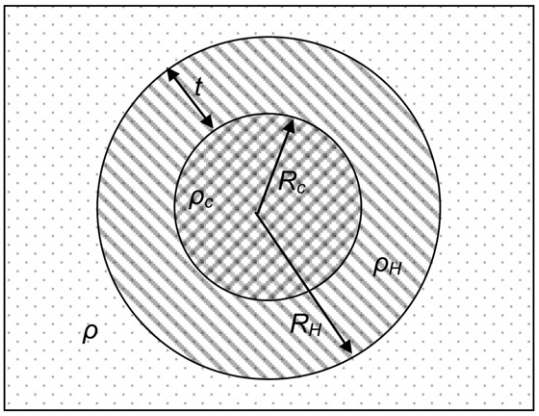

Fig. 1. Core–shell micelle with the core radius R_c, shell thickness t, micelle radius $R_s = t + R_c$, and the scattering length densities of the core, shell, and solvent, ρ_c, ρ_s, and ρ_o respectively.

Table 1
Molecular weights, degrees of polymerizations (DPn) and comonomer ratios (n/m) of $PDMA_m$–b–$PDEA_n$ diblock copolymers.

Sample code	$PDMA_m$–b–$PDEA_n$ diblock copolymers	DPn (m–n)	M_n g mol^{-1}	M_w g mol^{-1}	M_w/M_n	n/m
VB-I	$PDMA_{0.58}$–b–$PDEA_{0.42}$	70.0–51.0	20,380	21,600	1.06	0.72
VB-II	$PDMA_{0.67}$–b–$PDEA_{0.33}$	87.3–43.0	21,630	23,580	1.09	0.50
VB-II*	$PDMA_{0.67}$–b–$PDEA_{0.33}$	44.7–22.0	11,070	12,180	1.10	0.50
VB-III	$PDMA_{0.70}$–b–$PDEA_{0.30}$	84.7–36.3	20,000	22,400	1.12	0.43
VB-IV	$PDMA_{0.80}$–b–$PDEA_{0.20}$	98.4–24.6	20,000	21,590	1.08	0.25

Sample solutions were respectively sealed in 2-mm (X-ray path length) cells and measured at 23 °C, using a 10 keV beam of 0.5 mm diameter. One-dimensional SAXS profiles $I(Q)$ were circularly averaged from 2D images obtained using a MAR165 CCD detector. The scattering wavevector Q was calibrated with silver behenate [22]. The scattering intensity profiles $I(Q)$ were scaled to the absolute intensity units (cm^{-1}) using a high density polyethylene standard. The use of absolute intensity is necessary in extracting the aggregation number of the micelles form $I(Q = 0)$ values. All the SAXS data were corrected for detector noise, background scattering, incoming flux, and sample transmission [22]. DLS data were collected using the Malvern ALV/CGS-3 goniometer system (with ALV/LSE-5003 Multi-8-serial collector, $C\lambda_0$ = 632.8 nm, 22 mV, Helium-Laser); size and distribution of micelles were deduced from the observed scattering peak widths and positions.

4. Results and discussion

4.1. Effects of the n/m ratio

Fig. 3 shows the SAXS data for the $PDMA_m$–b–$PDEA_n$ copolymer, with n/m values in the range of 0.25–0.72, while keeping M_w ~22,000 and pH value ~7.6 at 23 °C. In such conditions, the SAXS data indicate formation of micelles for all the four cases. Using Guinier approximation (Fig. 3a) (Eq. (5)), the radius of gyration R_g (the square root of the average squared distance of each scattering particulate from its center) obtained for the micelles decreases systematically from 126 ± 5 to 113 ± 5, to 98 ± 4, to 85 ± 2 Å with n/m values decreased from 0.72, 0.50, 0.43, to 0.25. Assuming spherical micelles, the corresponding hydrodynamic radii deduced are 163, 146, 127, and 110 Å. Note that for spherical micelles, the hydrodynamic radius $R_H = (5/3)^{1/2}R_g$ or $R_g/R_H \approx 0.78$, which serves as an indicator for micellar shape [16]. The data can be fitted reasonably well using polydisperse spheres with the mean radius R_H and polydispersity p, as shown in Fig. 3b. From the fitted micelle size and calculated ρ_p (9.80 × 10^{-6} Å^{-2}) for the copolymer, we further deduce the aggregation numbers for the micelles, based on Eq. (2), neglecting the small C_o values (in general, smaller than 0.02 wt% as reported previously) [8]. Overall, the result shown in Fig. 3 indicates that increase of n/m value leads to higher hydrophobicity of the copolymer, hence, stronger tendency to aggregate with larger aggregation size and aggregation number.

We have also fitted the SAXS data in Fig. 3b with model shapes of rod and ellipsoid. The results indicate that polydisperse spheres, in general, can fit the data better. Nevertheless, the fitted parameters from these analytical model shapes of rod, ellipsoid, and polydisperse spheres, can converge roughly to similar dimensions. Therefore, we adopt the model of polydisperse spheres to interpret systematically all the SAXS data in this study. Small-angle X-ray or neutron scattering (SAXS or SANS) has been often used in revealing the size and shape of surfactant or polymer micelles of nanometer sizes [16]; although SAXS-determined sizes and shapes rely heavily on the non-unique model fitting result, structural information of nanometer micelles thus extracted provides valuable reference for micellar structures formed in delicately controlled solution environments that are otherwise difficult to access via imaging techniques. Moreover, the micelle sizes obtained from the SAXS data fitting are consistent with that from DLS, as show in Fig. 3; the corresponding sizes are summarized and compared in Table 2.

4.2. Effect of molecular weight

With the same pH, concentration, and n/m = 0.5 at 23 °C, but a reduced M_w ~12,000, the copolymer (VB-II*; cf. Table 1) could form compact micelles, as revealed by the characteristic core–shell hump of the SAXS data centered at Q ~0.07 Å^{-1} (Fig. 4). Note that the PDMA and PDEA blocks have differentiable scattering length densities (10.0 × 10^{-6} Å^{-2} and 9.7 × 10^{-6} Å^{-2}) for X-rays; the observable core–shell structure (discernable scattering contrast between the PDEA-core and PDMA-shell) suggests that the micellar core should form with more compact PDEA blocks, compared to the micellar corona or shell formed by the hydrophilic PDMA blocks stretching relatively well into the solvent. Using the core–shell model shown in Eq. (3), we could fit respectively the two sets of SAXS data of copolymer VB-II*, 10 and 20 mg mL^{-1}, adequately (solid curves in Fig. 4) with the same core radius of R_c = 52 ± 5 Å, shell thickness of t = 27 ± 3 Å (corresponding to a micelle radius $R_H = R_c + t$ = 79 Å cf. Eq. (3)); the fitted polydispersity is of a few percent (cf. Eq. (4)). The corresponding aggregation number N = 127 ± 15 is deduced based on the value of I_o, sample concentration, ρ_p and V_{dry} (9.80 × 10^{-6} Å^{-2} and 17,400 Å^3 for VB-II*), as that done previously. We have also fitted the same SAXS data with a core–shell ellipsoid model (dotted curve in Fig. 4); the best-fitted parameters with nearly identical major and minor axes support the model of spherical core–shell micelles of VB-II*. Compared to the aggregation behavior of the PDMA–b–PDEA copolymer VB-II, of the same n/m value but nearly two times larger M_w, the copolymer VB-II* apparently forms more compact micelles of a clearer core–

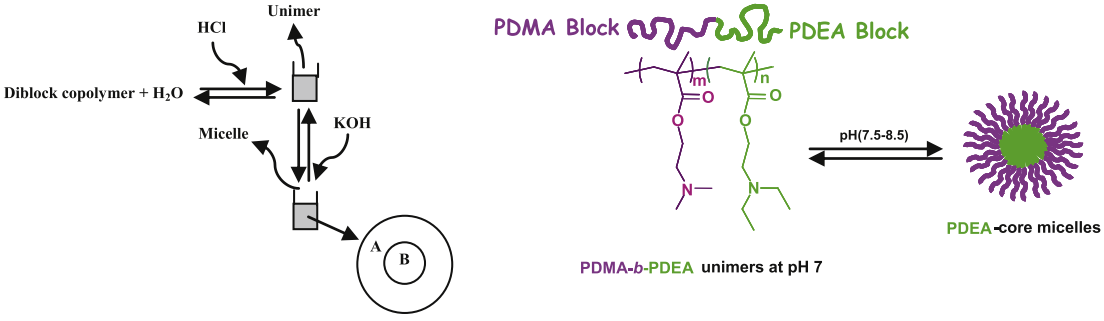

Fig. 2. Illustrations of sample preparation and micelle formation of PDMA–b–PDEA block copolymers at 23 °C. Note that A and B indicate PDMA and PDEA blocks, respectively.

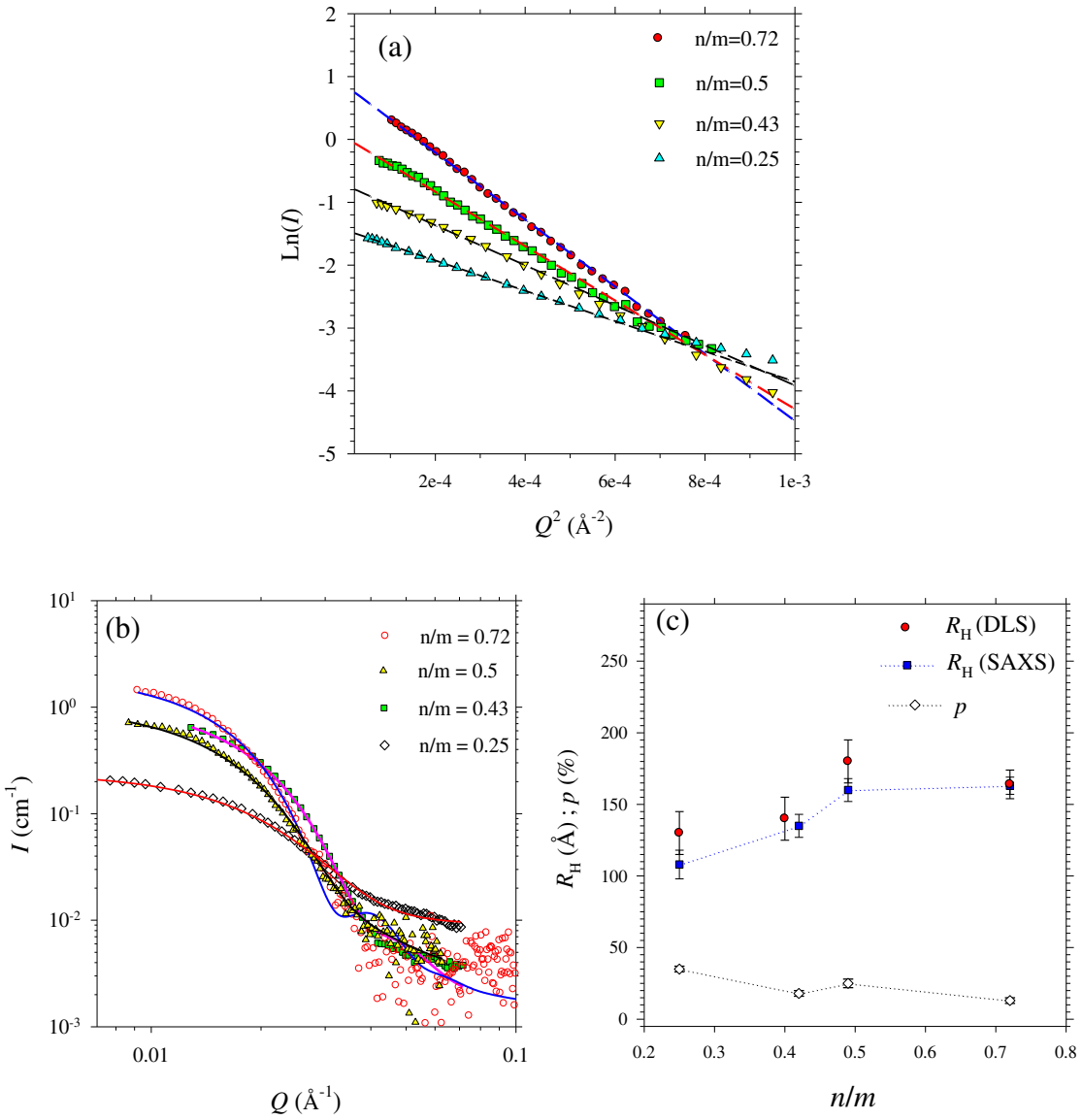

Fig. 3. (a) Guinier presentation for the SAXS data (fitted by the dotted lines) of the PDMA$_m$–*b*–PDEA$_n$ block copolymer, with different *n*/*m* values. (b) The same data are fitted (solid curves) using polydisperse spheres. (c) Micelle radii (R_H) and polydispersity *p* obtained from the data fitting. For comparison, consistent radii (within the error bars) obtained for the micelles from DLS are also shown.

shell structure (R_H = 80 Å of VB-II* vs. 146 Å of VB-II); presumably, the more dense chain packing provides a better scattering contrast for revealing the core–shell structure. The aggregation behavior may be explained in terms of the packing geometry of the copolymer, as detailed below. We note that there is a defect in the SAXS data fitting ($Q \sim 0.05$ Å^{-1}) for the higher concentration (20 mg mL^{-1}) case (Fig. 4), suggesting that the copolymer micelles might deviate slightly from the model of polydisperse spheres used. This deviation may be caused by a concentration effect; it is likely that more crowded micelles in the solution of 20 mg mL^{-1} induced stronger interactions and could not keep a constant shape all the time, leading to a smearing in shape-hence the difficulty in fitting the data with an analytical geometry form factor.

Table 2
SAXS and DLS results for Gunier radius R_g, (hydrodynamic) radius R_H, and aggregation number *N* of PDMA$_m$–*b*–PDEA$_n$ diblock copolymer micelles at solution pH = 7.6. $R_H = R_c + t$ for the core–shell micelle model with core radius R_c and shell thickness *t* is defined for VB-II*.

			SAXS			DLS
Sample	Conc. (M)	*n*/*m*	R_g (Å)	R_H (Å)	*N*	R_H (Å)
VB-I		0.72	126 ± 5	163 ± 10	252 ± 25	164 ± 15
VB-II		0.50	113 ± 5	146 ± 8	120 ± 12	180 ± 15
VB-II*		0.50	61 ± 8	79 ± 10	127 ± 15	71 ± 5
VB-II*			R_c = 52 ± 5; *t* = 27 ± 3			
VB-III		0.43	98 ± 4	135 ± 8	121 ± 12	140 ± 15
VB-IV		0.25	85 ± 2	108 ± 6	46 ± 5	130 ± 10

Previously, Borisov and Zhulina have also established a subtle model based on a mean-field theory for block copolymer micelles [23,24]. In the model, the free energy of the micelles is modeled in terms of the polymerization degrees of hydrophilic/hydrophobic blocks *m* and *n*, and several external parameters that control the interaction strength, hence the structure (chain conformation), in the hydrophilic corona of the micelles-including, for instance, the *effective* second virial coefficient related to the non-electrostatic excluded-volume interactions and the Coulomb interactions between the charged monomers. Minimizing the free energy leads to the structural properties, such as the aggregation number and

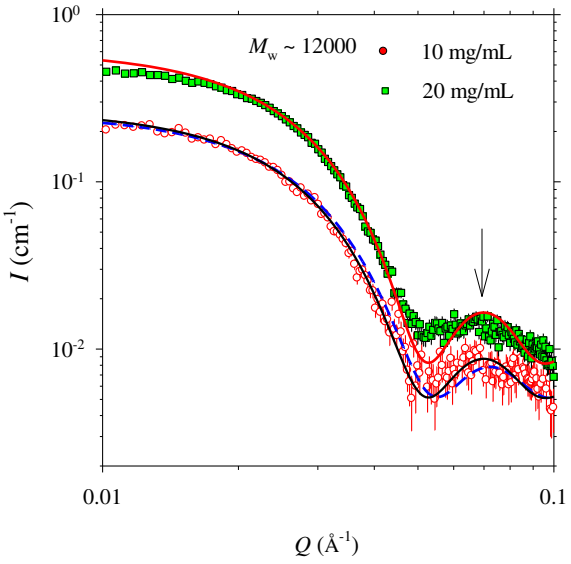

Fig. 4. SAXS data for the aqueous solutions of 20 and 10 mg mL^{-1} of PDMA–*b*–PDEA block copolymer VB-III, of a reduced M_w ~12,000. The arrow indicates the characteristic core–shell hump. The data are respectively fitted (solid curves) using the model of core–shell spherical (52 and 27 Å for the core radius and shell thickness) micelles. The slightly deviation of the fitting curve from the low-Q region data for the higher concentration solution is attributed to the small effect of interparticle interactions. For comparison, the fitting (dotted curve) with an ellipsoid shape (57 and 47 Å for the semi-major and semi-minor axes of the core and 27 Å for the shell thickness) deviate more from the data (10 mg mL^{-1}).

size, for equilibrium micelles. With the free energy expressions for spherical, cylindrical, or lamellar micelles, according to the respective packing geometries, morphological transitions of the micelles between these forms were predicted [23,24]. Especially, structural characteristics were elaborated based on the ratio ξ of shell-thickness-to-core-radius of copolymer micelles. With $\xi >> 1$ for star-like micelles, spherical form was shown to be favored thermodynamically; with $\xi << 1$ for crew-cut micelles, the increasingly larger repulsion in the corona might drive relatively easily a morphological transition to cylindrical or lamellar micelles for a better conformation entropy of the nonionic core blocks [23]. For the core–shell spherical micelles of VB-II* (shell thickness = 27 Å and core radius = 52 Å), ξ is ca. 0.5 (but not very much smaller than unity), implying a tendency for the spherical micelles to transit to, for instances, elongated rod-like or ellipsoidal micelles at higher micelle concentrations. This may be revealed by the less satisfactory SAXS data fitting for the higher concentration solution (20 mg mL^{-1}) with the spherical core–shell model, as shown in Fig. 4.

4.3. Effect of pH

An increase on solution pH directly enhances the degree of the deprotonation of the PDEA for stronger hydrophobicity, hence stronger aggregation tendency. Correspondingly, our DLS results reveal a behavior of increasing micellar size with increase of pH value (from 7.6 to 7.8) for the PDMA$_m$–*b*–PDEA$_n$ block copolymers (10 mg mL^{-1}) VB-II*; the micelle sizes obtained are summarized in Table 3. The larger micelles size at higher pH value is attributed to mainly the larger PDEA-core of higher aggregation number [2].

4.4. Effective packing parameter

Shapes of surfactant micelles are often predicted with the packing parameter [25,26] defined by

Table 3
DLS results for the pH-dependent micellar radii of PDMA$_m$–*b*–PDEA$_n$ diblock copolymers (10 mg mL^{-1}).

Sample	n/m	R_H (Å) pH = 7.6	R_H (Å) pH = 7.8
VB-II*	0.50	71	105

$$p = v_o/(a_o l) \quad (6)$$

with l for the aliphatic (hydrophobic) chain length and a_o the head group area of the surfactant; v_o is for the hydrophobic volume of the surfactant. For surfactants, spherical micelles form with $p < 1/3$, whereas rod micelles with $1/3 < p < 1/2$ and bilayers with $1/2 < p < 1$ [27]. For surfactants with small head groups, the values of v_o and l can be estimated rather well [27], and the aggregation structure and morphology transitions can be predicted closely from the packing parameter, once the value a_o is determined (depending on the interactions between the head groups in the relevant solution environment).

Here, we attempt to describe a copolymer micelle in terms of similar packing parameters used for surfactant micelles, as illustrated in Fig. 5. For copolymers, however, it is difficult to formulate the three corresponding parameters of the effective hydrophobic length l, head group area a_o, and hydrophobic volume v_o (Fig. 5). What not well-established are the estimations of the effective a_o and l values based on the copolymer molecular architecture such as the polymerization degrees of hydrophilic/hydrophobic blocks m and n, and the external parameters that control the interaction strength in the hydrophilic corona of the micelles [23,24]. Here, we attempt to correlate the structural characteristics of the copolymer micelles revealed by SAXS to a conceptual packing parameter analogous to that for surfactant micelles. Such correlations may be helpful in establishing empirical estimations for the effective a_o and l values for homologous copolymers.

Fig. 6 shows the growth behavior of aggregation number N obtained from SAXS for the studied PDMA–*b*–PDEA copolymers. The growth behavior of the aggregation number can be fitted well with an empirical relationship of $N \propto (n/m)^{1.6}$. Assuming the micelle core volume is filled completely, the aggregation number may be determined by

$$N = \left(4\pi l^3/3\right)/v_o \quad (7)$$

as suggested previously [28]. For copolymer micelles, the effective radius l depends on the chain configuration of the hydrophobic blocks in the solution and may be approximated by their end-to-end distance R_o in a form of $l \sim R_o = 2n^{\chi} l_c$ with the exponent χ

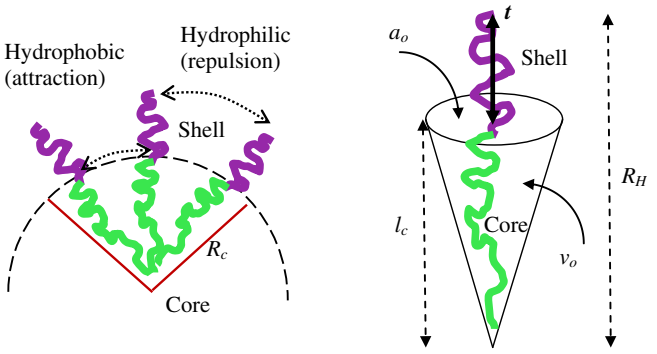

Fig. 5. Cartoons for a diblock copolymer micelle, characterized by the hydrophobic length l, junction area of the diblock copolymer a_o, micellar and core radii R_H and R_c, volume of the hydrophobic block of the diblock copolymer v_o.

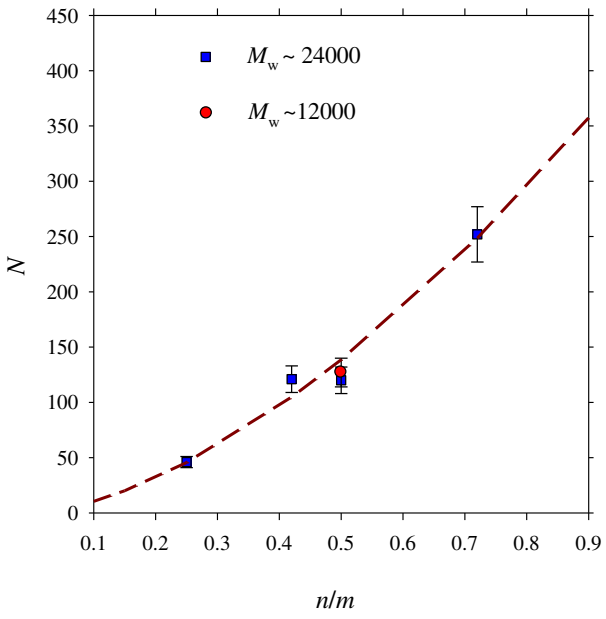

Fig. 6. Dependence of the aggregation number of the studied PDMA$_m$–b–PDEA$_n$ block copolymers (with two different M_w values as indicated) on n/m. All data are fitted with an empirical expression of $N = (n/m)^{1.6}$.

and a persistence length l_c. Here, χ describes the chain conformation in solution; $\chi = 0.5$ for Gaussian chain conformation and $\chi = 0.67$ for exclude volume chain conformation [29,30]. Since v_o is still linearly proportional to n, therefore, Eq. (6) leads to $N \propto n^{3\chi-1}$. Comparing this relation to the empirical fitted relation $N \propto (n/m)^{1.6}$, we obtain $\chi = 0.87$, suggesting that the PDEA blocks are relatively stretched (than excluded-volume chains) in forming the micelles cores. Furthermore, with the core–shell structure observed for VB-II*, we could estimate an a_o value of 260 Å^2, based on the core radius (52 Å) and aggregation number (127). Since the packing parameter requires $p < 1/3$ for the spherical copolymer micelles, the corresponding l value for the diblock copolymer should be larger than 73 Å, based on Eq. (5). Using $l \sim R_o = 2n^{\chi}l_c$ [28], with $n = 22$ (VB-II*), $\chi = 0.87$, we may deduce a persistence length $l_c > 2.5$ Å for the PDEA block. With the molecular structure of the PEDA block, the copolymer can easily fulfill the requirement of $l_c > 2.5$ Å, and form spherical micelles as observed.

We note that the aggregation number of PDMA–b–PDEA block copolymer micelles is also inversely linearly dependent on m, implying non-negligible effects from the hydrophilic PDMA blocks. Nevertheless, the exact relationship for a quantitative description of the hydrophilic PDMA blocks on the effective l or a_o value, hence the N value, is not easy to define quantitatively on a theoretical basis. Similar encountered with surfactant micelles are salt effects in screening charge interactions of the head groups, leading to complicate modulations in a_o-hence the micelle shape and aggregation number.

There are theoretical models, such as that given by Halperin [31], Nagarajan & Ganesh [32], or Zhulina et al. [33], that can include interactions and polymerization degrees of both the hydrophilic and hydrophobic blocks for predictions of copolymer micellization behavior. The empirical relation $N \propto (n/\mathrm{m})^{1.6}$ deduced for the aggregation number of the PDMA–b–PDEA block copolymer micelles is found to be relatively close to the prediction $N \propto n^2/\mathrm{m}^{1.5}$ of the model developed by Zhulina et al. for crew-cut micelles of neutral diblock copolymers [33]. The empirical relation for aggregation number, however, differs more from the model prediction by Nagarajan and Ganesh developed for micellization of diblock copolymers with marked amphiphilicity in a selective solvent [32].

5. Conclusion

Micellization behavior of the PDMA$_m$–b–PDEA$_n$ diblock copolymer have been investigated by using SAXS and DLS techniques. The micelle sizes of the block copolymer obtained from both SAXS and DLS studies are consistent. At the pH ranging 7.5–8.0 at ~23 °C, the diblock copolymer forms globular micelles; the aggregation number grows with $(n/m)^{1.6}$, regardless of the molecular mass. Reducing molecular mass leads to more compact micelles of a core–shell structure, with PDEA core radius of 52 Å, PDMA shell thickness of 27 Å, and aggregation number of 127. The deduced core–shell structure allows estimations of the effective hydrophobic/hydrophilic junction area a_o and hydrophobic length l of the copolymer in forming spherical micelles.

Acknowledgment

The authors would like to acknowledge NSRRC and SESAME for supports in SAXS measurements and the training program. UJ thanks TUBITAK (2221 Program) for supports during the collaboration stay in Turkey. VB thanks TUBA for the member support.

References

[1] O. Pillai, R. Panchagunia, Curr. Opin. Chem. Biol. 5 (2001) 447.
[2] B.C. Anderson, S.K. Mallapragada, Biomaterials 23 (2002) 4345.
[3] V. Bütün, S.P. Armes, N.C. Billingham, Chem. Commun. (1997) 671.
[4] V. Bütün, N.C. Billingham, S.P. Armes, J. Am. Chem. Soc. 120 (1998) 11818.
[5] V. Bütün, N.C. Billingham, S.P. Armes, J. Am. Chem. Soc. 120 (1998) 12135.
[6] V. Bütün, A.B. Loew, N.C. Billingham, S.P. Armes, J. Am. Chem. Soc. 121 (1999) 4288.
[7] V. Bütün, M. Vamvakaki, N.C. Billingham, S.P. Armes, Polymer 41 (2000) 3173.
[8] V. Bütün, S.P. Armes, N.C. Billingham, Polymer 42 (2001) 5993.
[9] V. Bütün, S.P. Armes, N.C. Billingham, Z. Tuzar, A. Rankin, J. Eastoe, R.K. Heenan, Macromolecules 34 (2001) 1503.
[10] A.S. Lee, A.P. Gast, V. Bütün, S.P. Armes, Macromolecules 32 (1999) 4302.
[11] A.S. Lee, V. Bütün, M. Vamvakaki, S.P. Armes, J.A. Pople, A.P. Gast, Macromolecules 35 (2002) 8540.
[12] I.W. Hamley, The Physics of Block Copolymers, Oxford University Press, New York, 1998.
[13] S.Y. Liu, J.V.M. Weaver, M. Save, S.P. Armes, Langmuir 18 (22) (2002) 8350.
[14] V. Bütün, F.F. Taktak, C. Tuncer, Macromol. Chem. Phys. 212 (2011) 1115–1128.
[15] M.V. Banez, K.L. Robinson, V. Bütün, S.P. Armes, Polymer 42 (2001) 29.
[16] S.H. Chen, T.L. Lin, in: K. Skod, D.L. Price (Eds.), Methods of Experimental Physics – Neutron Scattering in Condensed Matter Research, vol. 23B, Academic Press, New York, 1987 (Chapter 16).
[17] V. Castelletto, I.W. Hamley, Curr. Opin. Colloid 7 (2002) 167.
[18] U. Jeng, Y.S. Sun, H.Y. Lee, C.H. Hsu, K.S. Liang, S.W. Yeh, K.H. Wei, Macromolecules 37 (2004) 4617.
[19] U. Jeng, T.L. Lin, Y. Hu, T.S. Chang, T. Canteenwala, L.Y. Chiang, H. Frielinghaus, J. Phys. Chem. A 106 (2002) 12209.
[20] U. Jeng, C.S. Tsao, C.H. Lee, T.L. Lin, L.Y. Wang, L.Y. Chiang, C.C. Han, J. Phys. Chem. B 103 (1999) 1059.
[21] E.Y. Sheu, Phys. Rev. A 45 (1992) 2428.
[22] Y.H. Lai, Y.S. Sun, U. Jeng, J.M. Lin, T.L. Lin, H.S. Sheu, W.T. Chuang, Y.S. Huang, C.H. Hsu, M.T. Lee, H.Y. Lee, K.S. Liang, A. Gabriel, M.H.J. Koch, J. Appl. Crystallogr. 39 (2006) 871.
[23] O.V. Borisov, E.B. Zhulina, Macromolecules 36 (2003) 10029.
[24] O.V. Borisov, E.B. Zhulina, F.A.M. Leermakers, A.H.E. Müller, Adv. Polym. Sci. 241 (2011) 57.
[25] K. Holmberg, B. Jonsson, B. Kronberg, B. Lindman, Surfactant and Polymers in Aqueous Solutions, John Wiley & Sons Ltd, England, 2002, p. 60.
[26] J. Rodríguez-Hernández, Y. Chécot, F. Gnanou, S. Lecommandoux, Prog. Polym. Sci. 30 (2005) 691.
[27] R. Nagarajan, Langmuir 18 (2002) 31.
[28] A.B. Kayitmazer, D. Shaw, P.L. Dubin, Macromolecules 38 (2005) 5198.
[29] J.P. Cotton, D. Decker, B. Farnoux, G. Jannink, R. Ober, C. Picot, Phys. Rev. Lett. 32 (1974) 1170.
[30] U. Jeng, T.L. Lin, L.Y. Wang, L.Y. Chiang, D.L. Ho, C.C. Han, Appl. Phys. A 74 (Suppl.) (2002) S487.
[31] A. Halperin, Macromolecules 23 (1990) 2724.
[32] R. Nagarajan, K. Ganesh, Macromolecules 22 (1989) 4312.
[33] E.B. Zhulina, M. Adam, I. LaRue, S.S. Sheiko, M. Rubinstein, Macromolecules 35 (2005) 5330.